Application of a glutamate microsensor to brain tissue

Oldenziel, Weite Hendrik

Chapter 6

Monitoring extracellular glutamate in hippocampal slices with a microsensor.

This chapter is based on the following paper:

Oldenziel WH, Zeyden van der M, Dijkstra G, Ghijsen WEJM, Karst H, Cremers TIFH, Westerink BHC. Monitoring extracellular glutamate in hippocampal slices with a microsensor. *J. Neurosci Meth.* 2006, in press.

Abstract

The direct local assessment of glutamate in brain slices may improve our understanding of glutamatergic neurotransmission significantly. However, an analytical technique that monitors glutamate in brain slices is currently not available. Most recording techniques either monitor derivatives of glutamate or detect glutamate that diffuses out of the slice. Glutamate microsensors provide a promising solution to fulfil this analytical requirement. In the present study we have implanted a 10 µm diameter hydrogel-coated microsensor in the CA1 area of hippocampal slices to monitor extracellular glutamate levels. The influence of several pharmacological agents, which facilitate glutamate release from neurons or astrocytes, was investigated to explore the applicability of the microsensor. It was observed that KCl, veratradine, α-latrotoxine (LTX), $_{DL}$-threo-β-benzyloxyaspartate ($_{DL}$-TBOA) and l-cystine rapidly increased the extracellular glutamate levels. As far as we know this is the first study in which a microsensor is applied to monitor dynamic changes of extracellular glutamate in brain slices. Because the sensor monitors inside the slice in close proximity to cellular activity, it may contribute greatly to improve our understanding of the physiology of glutamatergic neurotransmission.

6.1 Introduction

l-Glutamate is the most abundant excitatory neurotransmitter in the central nervous system (CNS) and is involved in many aspects of normal brain functioning, e.g. in cognitive processes, motor behaviour, memory formation and in the development and plasticity of the CNS. In this respect, glutamate is also involved in the pathophysiology of many neurological, neurodegenerative and psychiatric disorders, such as epilepsy, Parkinson's disease, Alzheimer's disease, depression, stroke and schizophrenia (Cooper et al., 1996; Danbolt, 2001; Palucha and Pilc, 2005).

Recent studies have revealed that the physiology of glutamatergic neurotransmission in the CNS is mediated by a dynamic interplay between both neurons and astrocytes (Haydon 2001; Nedergaard et al., 2002; Volterra and Meldolesi, 2005). Advances in appropriate model systems and measuring techniques allow progress in unravelling the complexity of this physiology. An important research tool in this process is the use of brain slices. In contrast to *in vivo* experiments, brain slices allow a closer examination of cellular activity, experimental conditions can be better controlled and manipulations are easily performed (Gerhardt and Burmeister, 2000; Zimmer et al., 2000).

For a further understanding of glutamatergic neurotransmission, the direct assessment of extracellular glutamate with a high spatial and temporal resolution in the vicinity of synapses is required (Haydon, 2001). However, such a technique is currently not available. Most analytical techniques detect glutamate indirectly, for example by electrophysiological recordings of postsynaptic receptor or transporter currents (Jabaudon et al., 1999; Cavalier and Attwell, 2005), by optical bioimaging (Nakamura et al., 2003) or by ^{13}C NMR analysis (Sonnewald and Kondziella, 2003). These techniques often require additional interventions, e.g. application of receptor blockers, voltage-sensitive dyes or incubation with ^{13}C glutamate. The only techniques that detect glutamate itself are based on monitoring glutamate that diffuses out of the slice. Examples of such approaches are slices placed on sensor arrays (Kasai et al., 2001, 2002; Hirano et al., 2003; Qhobosheana et al, 2004), the use of superfusion or microperfusion systems (Waldmeier et al., 1993; Muzzolini et al., 1997), or placement of a microdialysis probe parallel to the slice (Robert et al., 1997). The most gentle approach used so far is the application of a capillary-based enzyme electrode, which is positioned approximately 60 µm above the slice

(Nakajima et al., 2003; Nakamura et al., 2005). Important to note is that the physiological significance of glutamate monitored outside the slice is questionable, as it has to escape first from the highly active reuptake processes before it is detected.

Glutamate microsensors represent a promising technique to monitor extracellular glutamate directly in brain slices. However, it appears that research concerning the application of a glutamate microsensor is still in its infancy. There are several technical difficulties in the construction and application of a microsensor (Niwa et al., 1996; Dale et al., 2005; Wilson and Gifford, 2005), which probably explains why glutamate microsensors have not been applied on a routine base in slice studies until now.

In recent years, we have given much attention to the construction and characterization of a 10 µm diameter hydrogel-coated glutamate microsensor (chapters 2-4), which was initially developed by Kulagina et al. (1999). In addition, we have evaluated the microsensor *in vitro* and *in vivo* (chapter 5). It appeared that due to its small dimensions (10 µm diameter) and advantageous analytical properties, in terms of response time, sensitivity, selectivity, linear range, etc, the microsensor was able to detect second-to-second changes of extracellular glutamate directly in brain slices. In the present study the microsensor was applied to monitor the effects of several compounds, which are known to affect glutamatergic neurotransmission, in order to further explore its potential as an analytical tool.

6.2 Experimental section

Animals and slice preparation

Male albino rats of a Wistar-derived strain (275-320 gr; Harlan, Zeist, The Netherlands) were decapitated (550020; Harvard Apparatus, Holliston, MA, USA) and the brain was rapidly removed and stored in ice-cold, continuously gassed (mixture of 95% O_2 / 5% CO_2), artificial cerebrospinal fluid (aCSF). After several minutes, transverse slices (400 µm) of the hippocampus were prepared with a tissue chopper (U0600; Proscitech, Kirwan, Australia). The slices were stored on a nylon mesh within a beaker, which contained continuously circulating, oxygenated (95% O_2 / 5% CO_2) aCSF at room temperature. The slices were stored at least 1 hr before use. The composition of the aCSF solution was (in mM): 124 NaCl, 3.5 KCl, 1.25 NaH_2PO_4, 1.5 $MgSO_4$, 2.0 $CaCl_2$, 2.5 $NaHCO_3$ and 10 glucose; pH 7.4 adjusted with sodium hydroxide. The aCSF solution was made in ultra-purified water (U.P.; Elgastat maxima, Salm en Kipp). The experiments were approved by the Animal Care Committee of the College of Mathematics and Natural Science of the University of Groningen.

Microsensor recordings in slices

A single slice was transferred to a recording chamber (21052; Fine Science Tools, Heidelberg, Germany). The slices were continuously perfused with aCSF (32-33°C, 3-5 ml/min) and kept fully submerged. The microsensor recordings were performed by implanting both a glutamate and background microsensor in close proximity (~ 200 µm; V-shaped form) in the CA1 area of the slice. The implantation procedure was visually controlled with a stereo microscope (Exacta-Optech, Diever, The Netherlands). The reference electrode (Ag/AgCl) was placed in the bathing solution of the recording chamber. The current output of both microsensors was monitored and after stabilization (~ ½ hr) different pharmacological agents were administered to the slice. Administration was performed by applying the drugs to the aCSF reservoir and perfusing the slice for a period of 10 min with this solution. Occasionally, a sequence of increasing drug concentrations was applied, in which each concentration was washed in for a period of 10 min. Some drugs (i.e. $_{DL}$-TBOA, TTX, CPG and LTX) were not washed in, but were administered directly in the bathing solution of the recording chamber. During this approach the rate of aCSF perfusion was decreased

to about 1 ml/min and after a short stabilization period (~ 5 min) at this particular flow rate the drugs were applied for a period of 10 min. Note, It was observed that the distribution of drugs was more difficult to control with this approach.

To estimate the *in situ* sensitivity of the sensor, experiments were performed in which exogenous glutamate was administered to the slice. Several assumptions had to be made to calculate this *in situ* sensitivity. For example, it was assumed that: a) exogenous glutamate diffused equally through the slice at both sides, b) implantation of the microsensor did not affect the diffusion of glutamate through the slice, c) the cellular uptake in hippocampal slices was similar to the cerebellar slices used by Garthwaite et al., (1992), and d) swelling of cells, due to exposure to glutamate, did not affect the diffusion of glutamate into the slice. Note, it is known that some of these assumptions are not always valid, but at present this is the closest approach to calculate the *in situ* sensitivity of the sensor.

Microsensors

Microsensors (glutamate- and background sensors) were constructed as previously reported (chapters 2 and 3). Briefly, carbon fiber electrodes (CFEs) with a diameter of 10 µm were trimmed to a length of 300-400 µm. The microsensors were prepared by coating the CFE with a five-component redox-hydrogel, in which l-glutamate oxidase, horseradish peroxidase and ascorbate oxidase were wired via poly(ethyleneglycol) diglycidyl ether to an osmium containing redox polymer (abbreviated as POs-EA). Application of a thin Nafion coating completed the construction.

The slice experiments were performed with two types of microsensors: glutamate and background sensors. The background microsensors were prepared similarly as the glutamate microsensors, only Glu-ox was not incorporated into the hydrogel. The studies were carried out by amperometrically operating the microsensor at a constant potential of –150 mV versus an Ag/AgCl reference electrode [0.15 M NaCl]. Before the microsensors were used in slice experiments, they were validated in a flow-injection analysis system (FIA; 1 ml/min), as described before in chapter 3.

After the slice experiments were finished, the microsensors were calibrated again at conditions mimicking the *in vitro* situation most closely. The sensitivity for glutamate was determined in continuously gassed (mixture of 95% O_2 / 5% CO_2) aCSF, at steady state conditions (i.e. aCSF perfusion at a rate of 0.1 ml/min in a FIA

system), in the presence of ascorbic acid 50 µM. This sensitivity was used to correlate the detected current (pA) to final extracellular glutamate concentrations. In addition, the drugs that were investigated in the slice experiments were also injected. None of the drugs induced an effect.

Chemicals

All components were obtained from Sigma-Aldrich (St. Louis, MO, USA), unless otherwise stated. $_{DL}$-threo-β-benzyloxyaspartate ($_{DL}$-TBOA) and (S)-4-carboxyphenylglycine (CPG) were obtained from Tocris Bioscience (Bristol, UK). Glutamate oxidase (Glu-ox; G-0400; 6.5 units/mg) was purchased from USBiological (Swampscott, MA, USA). Ascorbate oxidase was initially obtained form Seravac (Cape Town, South Africa; Product nr. 011530), but was purified prior to its use, as indicated in chapter 4. Salts, acetone p.a. and 2-propanol p.a. were obtained from Merck (Darmstadt, Germany**).** The calibration procedures of the microsensors were performed in aCSF, as reported previously (chapter 3). This aCSF, which was different from the aCSF applied for slices, had the following composition: 145 mM Na^+, 1.2 mM Ca^{2+}, 2.7 mM K^+, 1.0 mM Mg^{2+}, 152 mM Cl^- and 2.0 mM phosphate; pH 7.4 adjusted with sodium hydroxide. The aCSF solutions was made in UP-water. Enzyme solutions were made in HEPES buffer: the salt form of HEPES was added to a 10 mM solution of the acid form, until pH 8.

Statistics

Data are presented as mean ± SEM. The recordings of the microsensors (in pA) were averaged and represented as a black line (mean) with a gray area (SEM). The *n* number of each experiment represented the number of used slices. Each slice was obtained from a different animal and was investigated with a different set of microsensors. Sigmastat 3.0 was used to calculate statistics. Statistical analysis was performed using a Mann-Whitney Rank Sum Test on AUC and significance was set at $p < 0.05$. For statistical analysis the data (each second a data point) were averaged to sections of minutes and the output of both the glutamate and background microsensor at the different post-treatment minutes was compared to the minutes prior to the treatment.

6.3 Results

Microsensor recordings in the CA1 area

Experiments were conducted by placing both a glutamate and background microsensor in close proximity (~ 200 µm) in the CA1 area of a hippocampal slice. A typical example of the microsensors implanted in the CA1 region is shown in Fig. 1. The sensors were implanted through the whole thickness of the slice (~ 400 µm) to maximize the amount of contact. The current output of both microsensors was monitored and the difference in current was considered to represent the extracellular glutamate concentration ($[Glu]_0$). Several pharmacological agents were applied by a 10 min washing period and their influence on $[Glu]_0$ was investigated. The difference in current output between the glutamate and background microsensor prior to drug administration was set at 100% and was compared with the difference after drug administration.

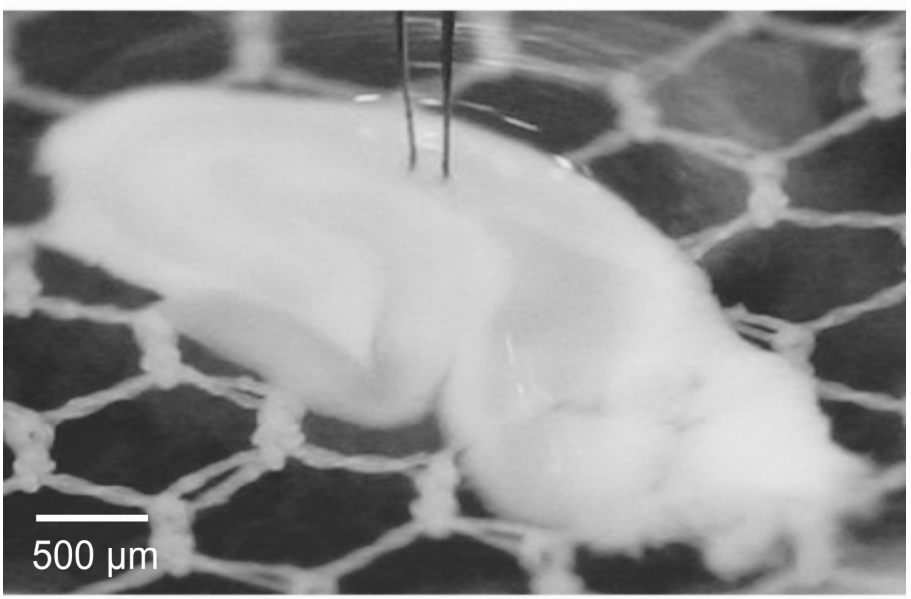

Figure 1: Insertion of a glutamate and background microsensor in the CA1 area of a hippocampal slice.

Extracellular glutamate levels

The output of the microsensors was monitored as current (pA). To correlate this current to final glutamate concentrations, it is necessary to calibrate the microsensor at conditions which are encountered in the slice (chapter 5), i.e. post *in vitro* calibration, at steady state calibration conditions, in the presence of approximately 50 µM ascorbic acid (AA) and 45 % pO_2. The sensitivity of the microsensor at these conditions was 5.0 ± 0.7 pA/µM (mean ± SEM; n = 19) and is indicated in the different figures.

This sensitivity is also used to quantify the basal extracellular glutamate concentration present in the slice. From an average of in total 209 experiments (performed with 55 sets of microsensors), the difference between the current output of the glutamate and background microsensor was 8.3 ± 4.8 pA (mean ± SEM), which correlates to a basal glutamate concentration of approximately 1.7 ± 1.0 µM.

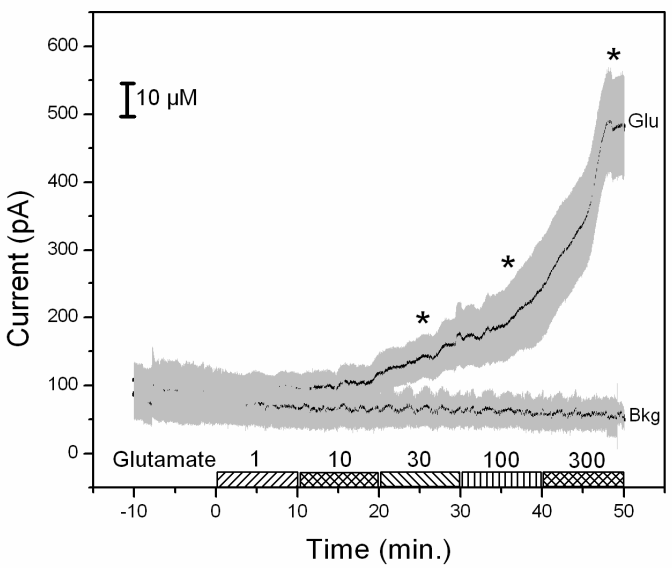

*Figure 2: Influence of exogenous glutamate on the detection properties of the glutamate (Glu) and background (Bkg) microsensor. A subsequent range of 1, 10, 30, 100 and 300 µM of exogeneous glutamate (n = 6) was applied to the slice and the glutamate levels in the slice were monitored. * Denotes a statistical significant difference between the microsensors (p < 0.05; Mann-Whitney Rank Sum Test).*

Monitoring glutamate release

To investigate whether the microsensors were capable of detecting extracellular glutamate in hippocampal slices, the influence of exogenous glutamate administration was investigated (Fig. 2). A subsequent range of 1, 10, 30, 100 and 300 µM of exogenous glutamate was administered in 10 min periods to the slice, which increased the detected glutamate levels dose dependently to 0, 2 (n.s.), 15, 30 and 83 µM respectively, as compared to the corresponding basal levels.

To further explore the potential of the microsensor, several drugs that are known to facilitate the release of glutamate were investigated. At first, the influence of a subsequent range of increasing KCl concentrations (30, 60 and 120 mM) was examined in the same slice (Fig. $3A_1$). The different concentrations increased $[Glu]_0$ dose-dependently to 6, 16 and 40 µM respectively. The different KCl concentrations were also investigated individually in different slices. It was observed that 30 mM (Fig. $3A_2$), 60 mM (Fig. $3A_3$) and 120 mM KCl (Fig. $3A_4$) increased $[Glu]_0$ dose-dependently to the same extent as observed in the subsequent range. Next, the influence of the sodium channel activator veratradine was investigated. Different concentrations (5, 10 and 50 µM) were investigated in the same slice (Fig. $3B_1$), which increased $[Glu]_0$ to about 1 (n.s.), 21 and 22 µM respectively. At the highest concentration the background sensor also displayed a slight response. In addition, the concentration of 50 µM was investigated individually (Fig. $3B_2$) and increased $[Glu]_0$ to approximately 25 µM. Third, the influence of the neurotoxin α-latrotoxine (LTX; 300 nM), which causes massive release of neurotransmitter pools, was investigated (Fig. 3C). LTX induced an increase in $[Glu]_0$ of 45 µM. In comparison to the other experiments, the results obtained with LTX displayed a higher variation, which most likely was due to the way of administration, i.e. application in the recording chamber next to the slice instead of a 10 min washing period. In Fig. 3D different concentrations (10, 100 and 500 µM) of the excitotoxin dl-cysteine were investigated, which increased $[Glu]_0$ to 2 (n.s.), 5 and 10 µM respectively.

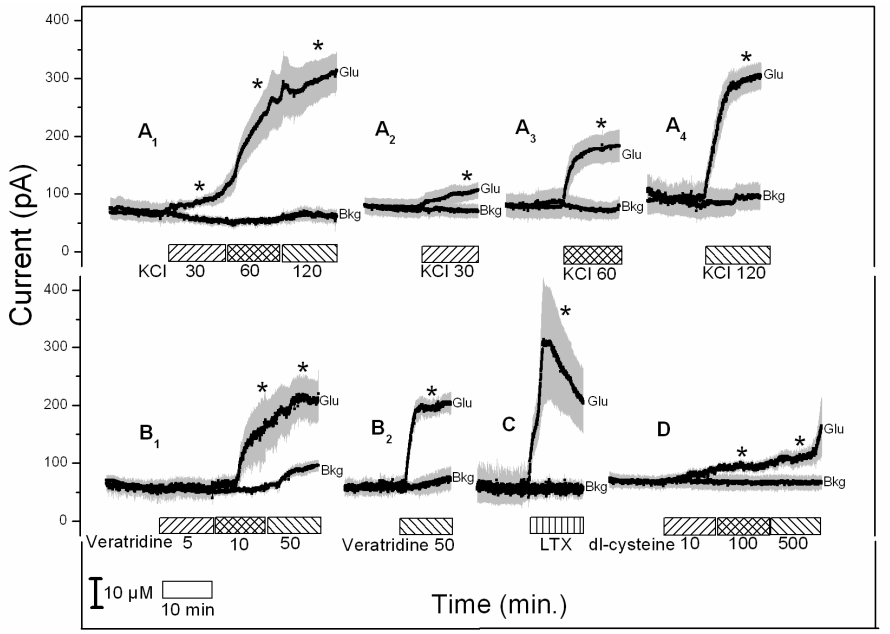

Figure 3: Influence of several pharmacological agents on the extracellular glutamate levels. ***A****) The influence of KCl on [Glu]$_0$.* ***A$_1$****) Range of 30, 60 and 120 mM KCl (n = 6).* ***A$_2$****) 30 mM KCl (n = 16).* ***A$_3$****) 60 mM KCl (n = 11).* ***A$_4$****) 120 mM KCl (n = 16).* ***B****) The influence of veratridine on [Glu]$_0$.* ***B$_1$****) Range of 5, 10 and 50 µM veratridine (n = 5).* ***B$_2$****) 50 µM veratridine (n = 5).* ***C****) Influence of 300 nM α-latrotoxine on [Glu]$_0$ (n = 5).* ***D****) Influence of 10, 100 and 500 µM dl-cysteine on [Glu]$_0$ (n = 5). * Denotes a statistical significant difference between the glutamate (Glu) and background sensor (Bkg) (p < 0.05; Mann-Whitney Rank Sum Test).*

Tonic release of glutamate

In order to show that the glutamate homeostasis is under tonic control inside the slices, the influence of the reuptake inhibitor $_{DL}$-threo-β-benzyloxyaspartate ($_{DL}$-TBOA) is shown in Fig. 4. It was observed that 200 µM of $_{DL}$-TBOA increased the glutamate levels approximately 7 µM (Fig. 4A). In Fig. 4B the effect of $_{DL}$-TBOA was investigated in combination with application of exogenous glutamate. First, the influence of 100 µM exogenous glutamate was examined (Fig. 4B$_1$), which increased the detected glutamate levels approximately 17 µM. Next, the slices were pre-treated with $_{DL}$-TBOA 200 µM for 10 min, followed by application of 100 µM glutamate (Fig. 4B$_2$). This induced an increase of the initial [Glu]$_0$ of approximately 38 µM.

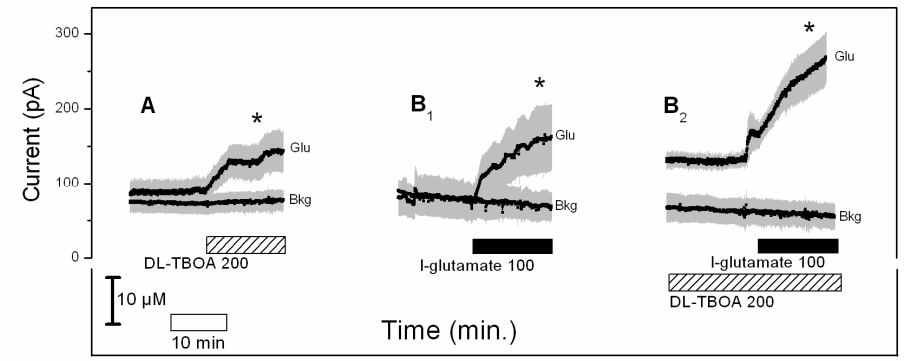

Figure 4: Influence of the reuptake inhibitor $_{DL}$-TBOA on the extracellular glutamate levels. ***A****) Application of 200 µM $_{DL}$-TBOA (n = 8).* ***B****) Influence of $_{DL}$-TBOA on the application of exogeneous glutamate.* ***B$_1$****) Application of 100 µM exogenous glutamate (n = 8).* ***B$_2$****) Pretreatment with 200 µM $_{DL}$-TBOA, followed by application of 100 µM exogenous glutamate (n = 7). * Denotes a statistical significant difference between the glutamate (Glu) and background sensor (Bkg) (p < 0.05; Mann-Whitney Rank Sum Test).*

For a closer examination of the tonic release of glutamate in the slice, the influence of several compounds was investigated. The influence of the sodium channel blocker tetrodotoxine (TTX; 20 µM) is shown in Fig. 5A. In Fig. 5B the influence of different concentrations (50, 200 and 500 µM) of the non-selective voltage-gated Ca^{2+} channel blocker cadmium chloride (Cd^{2+}) was examined. The influence of 4,4'-diisothiocyanatostilbene-2,2'-disulphonic acid (DIDS), a compound that blocks numerous anion transporters and channels and in particular pH-regulating transporters, was investigated in Fig. 5C. In addition, the influence of the glutamine synthetase inhibitor methionine sulfoximine (MSO; 5 mM) was investigated (n = 8; results not shown). However, none of these compounds appeared to effect $[Glu]_0$.

Recently, the cystine-glutamate exchanger has received much attention as a possible source of non-vesicular released glutamate (Baker et al., 2002, 2003). In Fig. 5D the influence of activation of the cystine-glutamate exchanger on the tonic release of glutamate was investigated in more detail. At first, the influence of different concentrations of l-cystine (10, 100 and 500 µM) was examined (Fig. 5D1), which increased $[Glu]_0$ dose-dependently to 1 (n.s.), 6 and 13 µM respectively. Next, the influence of different concentrations (10, 100 and 500 µM) of the cystine-glutamate exchange blocker homocysteic acid (HCA) was investigated (Fig. 5D2), which did not

alter $[Glu]_0$. In addition, when 500 µM l-cystine was applied after preincubation with HCA, no elevation of $[Glu]_0$ was observed. The same type of experiment was performed with (S)-4-carboxyphenylglycine (CPG; Fig. 5D3), which is another type of cystine-glutamate exchange blocker, but is also an antagonist of mGluR1 and mGluR5, and an agonist of mGluR2 metabotropic glutamate receptors. CPG (200 µM) did not influence $[Glu]_0$ and l-cystine did not increase $[Glu]_0$ when applied in combination with CPG.

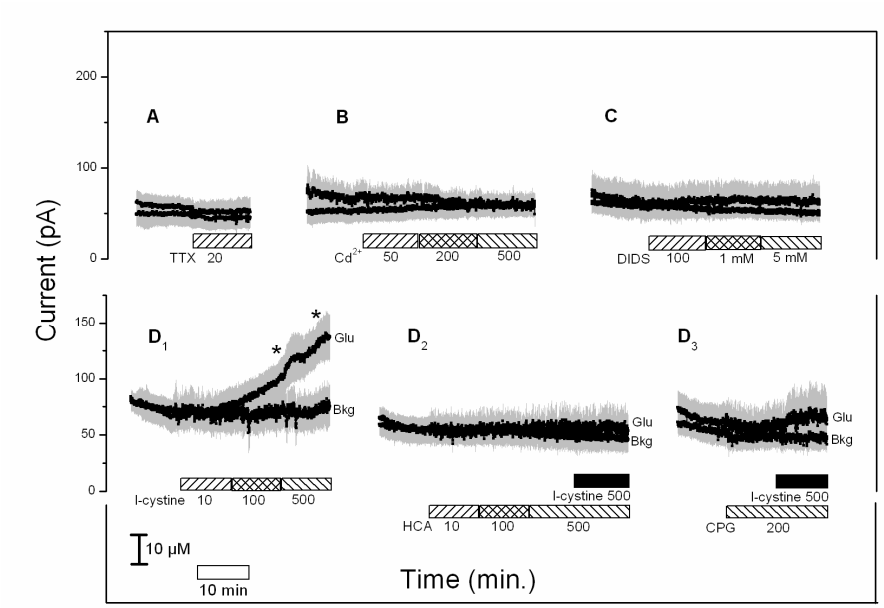

Figure 5: Influence of several pharmacological agents on the tonic release of glutamate. ***A****) 20 µM TTX (n = 6).* ***B****) Different concentrations (50, 200 and 500 µM) of Cd^{2+} (n = 5).* ***C****) Different concentrations (100 µM, 1 and 5 mM) of DIDS (n = 8).* ***D)*** *Influence of the cystine-glutamate exchanger on the tonic release of glutamate.* ***D_1****) Different concentrations of l-cystine (10, 100 and 500 µM; n = 7).* ***D_2****) Different concentrations of HCA (10, 100 and 500 µM; n = 6), followed by 500 µM l-cystine.* ***D_3****) Same experiment as in B), but now with 200 µM CPG, followed by 500 µM l-cystine. * Denotes a statistical significant difference between the glutamate (Glu) and background sensor (Bkg) (p < 0.05; Mann-Whitney Rank Sum Test).*

6.4 Discussion

Microsensor recordings in the CA1 area

In the present study the potential of the hydrogel-coated glutamate microsensor as an analytical tool in research on brain slices was evaluated. It appeared that its small dimensions (10 µm diameter) allowed implantation at a specific site of interest (high spatial resolution; Fig. 1), at which glutamate could be detected in the vicinity of cellular activity. For detection of extracellular glutamate levels both a glutamate and a background microsensor were used. The signal detected by the glutamate microsensor is derived from glutamate and from a non-specific electrochemical origin, whereas the background microsensor only detects the latter. Subtraction of both signals theoretically represents the extracellular glutamate concentration.

To investigate whether the microsensor was capable of detecting extracellular glutamate in a slice, different concentrations of exogenous glutamate were applied (Fig. 2). Application of glutamate induced a dose-dependent increase in detected glutamate levels. In addition, it is possible that endogenous glutamate also contributed to the signal, since glutamate addition can trigger the release of endogenous glutamate by exchange from cytosolic pools due to transporter reversal (Nedergaard, et al., 2002; Volterra and Meldolesi, 2005).

As the extracellular glutamate levels are detected as current (pA), an important question is how this current is related to actual glutamate concentrations. In chapter 5 we have observed that several crucial parameters significantly determined the performance of the microsensor. Calibration of the microsensor for these specific parameters is required, which in the slice are: biofouling (Wisniewski et al., 2000), steady state glutamate levels, approximately 45 % pO_2 (Jiang et al., 1991; Dean et al., 2003) and about 50 µM AA (Rice, 1999; Brahma et al., 2000). It appeared that the sensitivity of the microsensor for glutamate under these conditions was 5.0 ± 0.7 pA/µM. Complementary to this outcome, the sensitivity of the microsensor can also be estimated *in situ*, according the experiments in which different concentrations of exogenous glutamate are applied to the slice (Fig. 2 and Fig. $4B_1$). In a previous study it was demonstrated that the exogenous glutamate concentration detected by the sensor is an equilibrium between the diffusion of glutamate in the slice and a constant clearance by cellular uptake (Gartwaite et al., 1992), i.e. the deeper inside the slice, the lower the concentration of glutamate, until a depth is reached at which

the rate of cellular uptake exactly balances the rate of inward diffusion of glutamate. According to this report it can be calculated that the *in situ* sensitivity of the microsensor for 100 µM glutamate will be approximately 12.3 ± 5.0 pA/µM (Fig. 2) or 8.3 ± 3.3 pA/µM (Fig. $4B_1$) and for 300 µM glutamate it will be about 7.0 ± 1.2 pA/µM (Fig. 2). These values agree fairly well with the determined sensitivity by post *in vitro* calibration. Several assumptions had to be made for these calculations, as referred to in the Materials and Methods section.

It is important to note that glutamate was monitored while drugs were washed in during periods of ten minutes. Therefore the diffusion characteristics of the studied compounds into the slice contributed importantly to the temporal resolution of the microsensor. At present, experiments are in progress in which local glutamate transients are monitored inside the slice upon electrical stimulation and local application of small aliquots of drugs. It is obvious that in such experiments the temporal resolution of the sensor will become more important.

Monitoring glutamate release

The potential of the microsensor was further explored by applying different pharmacological agents, which are known to facilitate the release of glutamate via different mechanisms: KCl, veratradine, LTX and dl-cysteine (Fig. 3). First, different concentrations of elevated [K^+] were applied, which induced a dose-dependent increase in extracellular glutamate. The results agreed with preliminary microsensor data (Hu et al., 1994; Oldenziel et al., 2006b (chapter 5)), but were much higher than observed with other recording techniques, such as superfusion, microdialysis, or capillary-based electrode systems (Takashi and Hashimoto, 1996; Robert et al., 1997; Nakajima et al., 2003). Probably, the detected glutamate originates both from neurons and astrocytes, as high [K^+] causes depolarisation of neurones, which results in vesicular release of glutamate (Katsumori et al., 1999; Waagpetersen et al., 2005), whereas glutamate is released from astrocytes as part of the internal cell volume regulation (Kimelberg et al., 1995; Leis et al., 2005). The latter is primarily controlled by the type 1 electroneutral Na-K-Cl cotransporter (NKCC1; Chen and Sun, 2005).

Next, it was observed that different concentrations of the alkaloid veratradine induced significant increases in extracellular glutamate. Comparable elevations were reported previously with slice perfusion studies (Roettger and Lipton, 1996; Bianchi et al., 1999). Likely the detected glutamate originates from neurons, as veratridine

enhances the influx of sodium through voltage sensitive sodium channels, which in turn causes neuronal depolarization and release of glutamate from vesicles and the cytosolic pool (Alkadhi and Tian, 1996; Tikonov and Zhorov, 2005).

Third, a large increase in extracellular glutamate was induced by the potent neurotoxin LTX. The detected glutamate is most likely derived from vesicular origin, as LTX acts selectively on presynaptic nerve terminals and induces exocytosis via a complex mechanism (Ashton et al., 2001; Hlubek et al., 2003), which involves activation of presynaptic receptors (neurexin and latrophilin receptors), insertion of the toxin into the membrane and subsequent pore formation (Ashton et al., 2001; Hlubek et al., 2003). As far as we know, the influence of LTX on extracellular glutamate levels has not been investigated before in slice studies.

Finally, small and slowly occurring increases in extracellular glutamate were observed after application of the amino acid dl-cysteine. The observed increases in glutamate were much higher as previously reported in superfusion studies (Janáky et al., 2000). The l-isomer of dl-cysteine is an excitatory agent and is thought to evoke the release of glutamate via three possible mechanisms: inhibition of the uptake of glutamate, the production of free radicals (e.g. hydrogen peroxide and S-nitrocysteine), which in turn may stimulate the release or inhibit the uptake of glutamate, and inhibition of glutamate decarboxylase, which allows extracellular accumulation of glutamate (Abbas et al., 1997; Janáky et al., 2000). At present it is not known if the d-isomer also exerts an effect.

It is concluded that the microsensor is able to monitor the release of extracellular glutamate from various physiological origins. When compared to other recording techniques it is apparent that the detected signals are relatively large, which is explained by the fact that the microsensor monitors inside the slice (with a high sensitivity), in close proximity of cellular activity.

Tonic release of glutamate

An average difference of 8.3 ± 4.8 pA was observed between the glutamate and background microsensor, which correlates to a $[Glu]_0$ of approximately 1.7 ± 1.0 µM. However, this value should be interpreted with caution, as a slight variation in the basal current output of both microsensors also contributed to the recordings. Small differences in slices, sensors and experimental conditions may induce such a variation. This also explains why no distinguishable difference was observed between

the average current output (mean ± SEM) of both sensors in most experiments, whereas in each individual experiment the current output of the glutamate microsensor was higher compared to the output of the background sensor. In addition, an overestimation of the basal signal might occur as the (outer) cells of the slice possibly release glutamate as part of dying and damaging processes.

The reuptake inhibitor $_{DL}$-TBOA was used to investigate the tonic release of glutamate in slices in more detail. $_{DL}$-TBOA, which is a blocker of the glutamate transporters EAAT1-3, induced a clear increase in extracellular glutamate levels. This suggests a dynamic equilibrium between the basal tonic release and active reuptake of glutamate, although a contribution of actively released glutamate from astrocytes by heteroexchange can not be ruled out completely, as the non-transportable $_{DL}$-TBOA partly behaves as a transportable inhibitor on astrocytes (Anderson et al., 2001). In addition, it was observed that application of exogenous glutamate in the presence of $_{DL}$-TBOA induced significantly higher glutamate levels, which indicates that the diffusion of glutamate through the slice is facilitated by blocking the reuptake sites. This also indicates that blocking the highly active reuptake mechanisms, as often occurs as a standard procedure within *in vitro* research (e.g. Jabaudon et al., 1999; Cavalier and Attwell, 2005), drastically changes the physiological context. Consequently, the relevance of results obtained at such conditions should be interpreted with caution.

Despite the fact that the difference between the glutamate and background sensor was small, an attempt was made to further elucidate the origin of tonically released glutamate. Three main sources were considered: glutamate released from neurons, from astrocytes and from passive diffusion of glutamate across cell membranes. The first was investigated by applying TTX and Cd^{2+}, the second by infusing DIDS and several compounds which affect the cystine-glutamate exchanger (i.e. l-cystine, HCA, CPG and a combination of these drugs), and the third by infusing MSO.

It was observed that none of these compounds affected the tonic release of glutamate, although Cd^{2+} tended to induce a small decline. An interesting observation was that l-cystine induced a dose-dependent increase in extracellular glutamate levels, which could be blocked by the inhibitors HCA and CPG, whereas the blockers itself did not affect basal $[Glu]_0$. This implies that the cystine-glutamate exchange activity is present in the slice and that it can contribute to the release of glutamate

when the extracellular l-cystine concentration exceeds a certain level. However, this level is probably higher than the basal l-cystine extracellular concentration.

It is concluded that in the present study we were not able to elucidate the origin of $[Glu]_0$ in slices. This can be explained as follows. First, we only have investigated a few possible sources of glutamate release, whereas many different mechanisms of release are known (Nedergaard et al., 2002; Cavalier et al, 2005; Volterra and Meldolesi, 2005). In addition, the difference in current output between the glutamate and background microsensor is small and close to the limit of detection. All the experiments in this study were performed to detect a wide range of effects. However, it is likely that for a closer examination of the origin of tonically released glutamate, the experiments need to be carried out with a more specific focus. At present, these aspects are under investigation. Another question, which has not has received any attention in this study, is the release of glutamate due to spontaneous activity. At present it is not known if this contributes to the tonic release of glutamate and if the sensor is able to record such activity. Experiments in which electrophysiological recordings are combined with microsensor recordings are in progress to study this in more detail.

6.5 Conclusion

It is concluded that the microsensor forms a promising analytical tool for local monitoring of extracellular glutamate in brain slices. The high temporal and spatial resolution of the microsensor allows a second-to-second monitoring of glutamate at specific sub areas of the slice. Moreover, because the microsensor monitors in the vicinity of cellular activity, it most likely detects physiological processes to a larger extent as compared to techniques that monitor glutamate outside the slice. This probably explains why the relative effects detected with the microsensor are much higher compared to other recording techniques. An additional advantage is that experimental conditions and manipulations can be controlled easily. This allows the possibility of combining the microsensor with complementary techniques, such as electrophysiological recordings and electrical stimulation. This will generate an even more powerful approach and currently these experiments are in progress.